analytical chemistry

Article

pubs.acs.org/ac

Selective Naked-Eye Detection of Hg^{2+} through an Efficient Turn-On Photoinduced Electron Transfer Fluorescent Probe and Its Real Applications

Priyanka Srivastava,[†] Syed S. Razi,[†] Rashid Ali,[†] Ramesh C. Gupta,[†] Suresh S. Yadav,[‡,§] Gopeshwar Narayan,[‡,§] and Arvind Misra*[,†]

[†]Department of Chemistry, Faculty of Science, Banaras Hindu University, Varanasi 221005 Uttar Pradesh, India

[‡]Department of Molecular and Human Genetics, Faculty of Science, Banaras Hindu University, Varanasi 221005 Uttar Pradesh, India

Supporting Information

ABSTRACT: A simple molecular fluorescent probe **5** has been designed and synthesized by appending anthracene and benzhydryl moieties through a piperazine bridge. The probe upon interaction with different metal ions showed high selectivity and sensitivity (2 ppb) for Hg^{2+} through fluorescence "turn-on" response in HEPES buffer. The significant fluorescence enhancement (~10-fold) is attributable to PET arrest due to complexation with nitrogen atoms of the piperazine unit and Hg^{2+} in 1:2 stoichiometry, in which a naked-eye sensitive fluorescent blue color of solution changed to a blue-green (switched-on). As a proof of concept, promising prospects for application in environmental and biological sciences **5** have been utilized to detect Hg^{2+} sensitively in real samples, on cellulose paper strips, in protein medium (like BSA), and intracellularly in HeLa cells. Moreover, the optical behavior of **5** upon providing different chemical inputs has been utilized to construct individual logic gates and a reusable combinational logic circuit. The combinational circuit (switch ON mode; OR logic gate) is easily resettable to the original position (switch OFF mode; INHIBIT logic gate) by applying reset chemical inputs (OH^- and PO_4^{3-}) with great reproducibility.

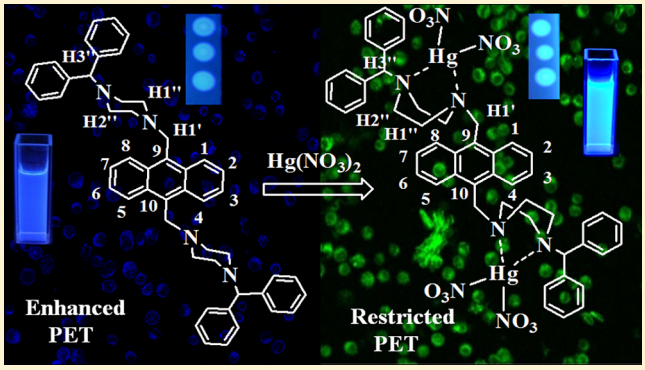

Recently, heavy and transition metal (HTM) contamination has brought forth serious environmental and health problems.[1] Among HTMs, mercury (Hg^{2+}) is recognized as a detrimental neurological toxin which is widely distributed in the environment by various natural processes, industrial releases, and anthropogenic activities.[2,3] The bioaccumulation of such toxic material in living tissues of human and animal bodies via a food chain causes mercury poisoning, serious neural disorder, and diseases like Minamata.[1−3] The Environmental Protection Agency (EPA) has set a 2 ppb maximum tolerable level of mercury contamination in drinking water.[2,3] Therefore, considerable current interest has arisen to develop selective and sensitive methodologies for the detection of HTMs owing to their extensive use and ensuing impact on the environment.

Many reports dealing with the detection of Hg^{2+} show fluorescence quenching[2] because Hg^{2+} is known to induce a spin−orbit coupling effect and is spectroscopically and magnetically silent (filled d^{10} orbitals).[4] Therefore, the common analytical techniques such as nuclear magnetic resonance (NMR) and electron paramagnetic resonance (EPR) are not adequately competent to detect Hg^{2+} in environmental and biological systems. Optical based techniques (fluorescence, phosphorescence, and chemiluminescence) have some obvious real time advantages since they are simple, noninvasive, and highly sensitive.[1] Moreover, progress in development of naked-eye sensitive chemosensors for the detection of HTM ions are increasingly appreciated important aspect since it may offer qualitative and quantitative information. Mercury mediated chemical reactions such as deselenation, hydrolysis, mercuration, and also coordination to sulfur containing receptors are some common strategies to develop good fluorescent sensors for mercury;[5,6] however, systems capable to detect Hg^{2+} through enhanced fluorescence are rare.[7] While looking for a good sensor motif, particularly for Hg^{2+}, the major concern is to achieve good optoelectronic properties, "turn-on" emission, as well as naked-eye sensitive color changes. In contrast to "turn-off" motifs, "turn-on" emission is preferred to enhance detection sensitivity and ease low concentration detection with negligible background. Moreover, the aqueous medium compatibility is another limiting factor and the fluorescence probes to detect Hg^{2+} in pure or partial aqueous medium are limited in number.[8−13] Thus, the development of facile and

Received: May 5, 2014
Accepted: August 6, 2014
Published: August 6, 2014

   dx.doi.org/10.1021/ac501780z | *Anal. Chem.* 2014, 86, 8693−8699

efficient methodologies to detect Hg^{2+} in the environment and living systems through enhanced emission is a continuing endeavor among the scientific community, including biologists and environmentalists.

Keeping in mind the paramount importance of achieving high affinity and selectivity for Hg^{2+}, we herein report a new sensor motif to detect the Hg^{2+} through a fluorescence "turn-on" response in partial aqueous medium (10 mM; HEPES buffer pH 7.0; ACN/H_2O 3:7, v/v). While synthesizing an innovative rational synthetic typical sensor motif, we incorporated anthracene core as a fluorescent signaling unit along with two benzhydryl moieties and piperazine units as a suitable ionophore to coordinate Hg^{2+} selectively. We assumed that as a soft closed-shell cation Hg^{2+} has a pronounced affinity to nitrogen-donor ligands, as in the case of classical azacrown ethers[14] and simple piperazine (pK_a, 9.8) unit would promote a stable 1:2 complexation with mercuric salts in aqueous medium, without interference of competitive metal ions.[14] Second, the introduction of benzhydryl and anthracene moieties in conjugation to piperazine will form a more stable hydrophilic photoinduced electron transfer (PET) chemosensor[15] by acquiring a thermodynamically favorable minimum energy configuration. As a proof of concept, the molecular probe **5** has shown high sensitivity to detect Hg^{2+} in real samples, on cellulose paper strips, and protein medium like BSA. Intracellular fluorescence imaging of Hg^{2+} was also realized in HeLa cells.

EXPERIMENTAL SECTION

Detection of Hg^{2+} in Real Contaminated Water Samples. To accomplish, a real crude water sample (50 mL) was passed through a microfiltration membrane and the pH of the sample was adjusted using HEPES buffer. The aliquots of water samples were mixed with accurately prepared different concentrations of Hg^{2+} (0.02, 0.2, 2 μM). The resulting samples then treated with **5** in HEPES buffer (pH, 7.0) to obtain final mixtures (3 mL) containing an accurate concentration of probe **5** (10 μM) and Hg^{2+} ions (0.02, 0.2, 2 μM). The samples were left for 5 min, and fluorescence spectra were measured in triplicates.

Live Cell Imaging and Cell Viability Test. HeLa cells were cultured in Dulbeco's modified eagle medium (DMEM) supplemented with 10% fetal bovine serum (FBS), 1% antibiotics, and antimycotic (Himedia) and incubated overnight at 37 °C in the environment of CO_2 (5%) as per manufacturer's protocol. Probe **5** (40 μM) was dissolved in a culture medium containing 0.1% (v/v) DMSO and incubated into the cells for 30 min at 37 °C. As a control experiment, the cells were pretreated with PBS or *N*-methylmaleimide (NMM, 500 μM) for 1 h, then washed (5 min, two times) with 1×PBS buffer (pH 7.4) and incubated with **5** (10, 20, 30, 40, 50 μM) in the cultured media containing 0.1% (v/v) DMSO. After 30 min of incubation, cell images were acquired under a fluorescence microscope.

To study the cytotoxicity, HeLa were seeded in a 96-well plates (5 × 10^3cells/well) in duplicate and were cultured in complete DMEM medium. HeLa cells were incubated separately with different concentrations of probe **5** (10, 20, 30, 40, 50 μM) and probe **5** with $HgNO_3$ (1 μM) for 24 h. To determine cell viability, the colorimetric metabolic activity assay was performed by incubating treated cells with 3-(4,5-dimethylthiazol-2-yl)-3,5-diphenyltetrazolium bromide (MTT) (5 mg/mL MTT reagent in PBS) for 2 h. The insoluble purple formazan crystals, obtained by the reduction of yellow tetrazolium salt (MTT) on metabolically active cells, were dissolved with the help of DMSO (Sigma). The color was quantified spectrophotometrically on a microtiter plate reader (Bio-Rad model 680 microplate reader) at 380 nm excitation. Each experiment was repeated for three times. The cytotoxic effect of the probe was assessed through the ratio of the absorbance of the probe treated sample versus the control sample. The confocal microscopic images were recorded on an LSM 510 Meta Confocal microscope (20× Zeiss objective lens). To collect confocal microscopic images, HeLa cells were treated separately with a 40 μM solution of probe **5** and **5** + $HgNO_3$ in the dark and washed twice for 5 min with 1× PBS buffer (phosphate saline, pH 7.4). Cells were recollected by centrifugation (at 2000 rpm for 2 min) and mounted on slides with the help of DABCO.

RESULTS AND DISCUSSION

Probe Design and Photophysical Studies. The synthetic route adopted for preparation of **5** is shown in Scheme 1. In a sequence of reactions,[16] the benzophenone unit

Scheme 1. (i) $NaBH_4$/Ethanol, (ii) $SOCl_2$/DCM, (iii) Piperazine/K_2CO_3/DMF, (iv) Paraformaldehyde/HCl/Dioxane, and (v) 3/K_2CO_3/DMF

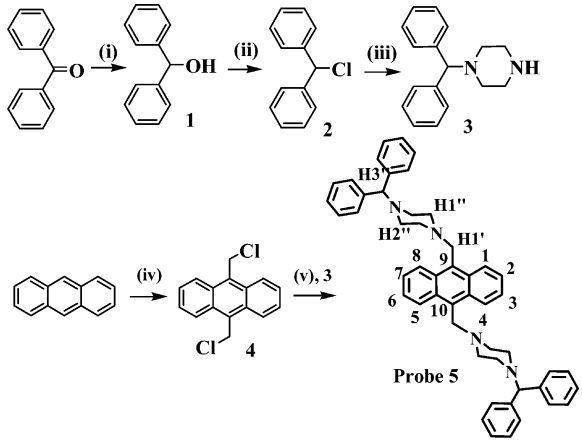

was first reduced with sodiumborohydride and subsequently reacted with thionyl chloride to get chloromethyl benzhydryl, **2**, in good yield. Compound **2** was refluxed with piperazine in DMF to get **3** in 80% yield.[16] Anthracene was treated with paraformaldehyde and hydrochloric acid to get bischloromethylanthracene **4** in good yield (~38%). Compounds **3** and **4** were reacted under anhydrous conditions in the presence of K_2CO_3 in DMF to yield probe **5** (85%) as a light yellow color powder. The chemical structures were well characterized and data are given as Supporting Information (see Supportive Information Figures S1−S7).

The aqueous medium compatibility of probe **5** enabled photophysical investigation in HEPES buffer (10 mM pH 7.0; ACN/H_2O 3:7, v/v). The electronic transition spectrum of **5** (50 μM) showed typical absorption bands at 395, 374, and 355 nm. Probe **5** (10 μM) at 376 nm excitation displayed very weak broad emission bands of low quantum yield (Φ = 0.001 with respect to quinine sulfate) at 402 and 422 nm, which is attributed to the photoinduced electron transfer (PET) process (Figure 1). Since the designed probe has nitrogen atoms on the bridging piperazine unit, it is expected to show variable optical

dx.doi.org/10.1021/ac501780z | Anal. Chem. 2014, 86, 8693−8699

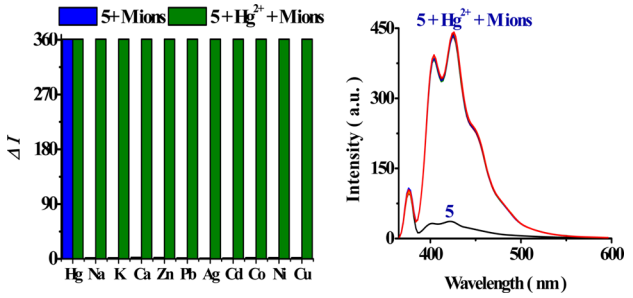

Figure 1. Bar diagram shows change in emission intensities of **5** and a complex, **5**−Hg^{2+} upon interference of tested cations in HEPES buffer (10 mM; pH 7.0; 70% H_2O−ACN). Inset: Emission spectra of **5** and its complex, **5**−Hg^{2+} upon interference of tested cations.

behavior at different pHs. The pH dependent photophysical studies were performed in HEPES buffer. Notably, the resulting absorption and emission spectra of **5** have shown pH insensitivity in the range 7−14. However, in the acidic medium (pH 1−6.5), absorption spectra showed marginal hypochromicity along with a blue-shift of 3 nm while significant fluorescence enhancement with a bathochromic shift of 8 nm (Figure S8a,b in the Supporting Information). This is attributable to protonation of nitrogen atoms of the piperazine unit of **5** which restricts the PET (PET-Off). The distribution of **5** in a broad pH range suggested protonation of **5** below pH ≤ 6.0 while remain unaffected at neutral to alkaline pH (pH ≥ 6.0) (inset of Figure S8b in the Supporting Information). Therefore, **5** can be utilized as an appropriate probe to work at physiological pH (pH 7.0).

Sensitivity and Selectivity of Probe 5 to Detect Hg^{2+}. Upon interaction with Hg^{2+}, the absorption spectra of **5** displayed a bathochromic shift of ∼3 nm along with a marginal decrease in molar absorptivity. In contrast, the emission spectra of **5** (λ_{ex} = 376 nm) upon interaction with Hg^{2+} exhibited fluorescence "turn-on" response in which relative emission intensity was enhanced, ∼10.5-fold with a red shift of 2−4 nm (Figure S9 in the Supporting Information) and the color of solution "switched-on" to a fluorescent blue-green from a fluorescent blue color (inset of Figure 2). The other tested metal ions (such as Na^+, K^+, Ca^{2+}, Zn^{2+}, Pb^{2+}, Ag^+, Cd^{2+}, Co^{2+}, Ni^{2+}, and Cu^{2+} (5.0 equiv) failed to exhibit any significant change in the photophysical behavior of **5**. Therefore, this

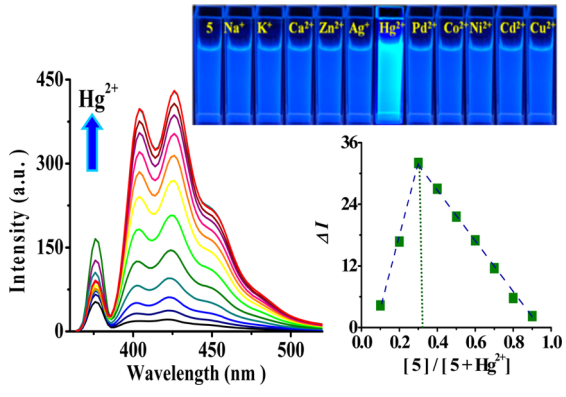

Figure 2. Emission titration spectra of probe **5** upon addition of Hg^{2+} (0−5 equiv) in HEPES buffer (10 mM; pH 7.0; 70% aqueous−ACN). Inset: change in color of **5** upon interaction with tested cations. Jobs plot for a 1:2 stoichiometry.

suggested high sensitivity and selectivity of probe **5** for Hg^{2+} ions. Moreover, the metal ions interaction studies were also performed in PBS buffer (10 mM; pH 7.0) and an acetonitrile−water gradient system (70%; 3:7; v/v). Probe **5** showed insignificant change in the emission behavior in PBS buffer, however, in an ACN−H_2O gradient system emission intensity of **5** was relatively high as compared to emission observed in HEPES buffer. Also upon interaction with metal ions probe **5** in ACN−H_2O showed almost similar binding behavior with Hg^{2+} with relatively enhanced emission intensity (∼15%) (Figure S10 in the Supporting Information). Therefore, it is worth to mention that probe **5** is suitable to detect Hg^{2+} in ACN−H_2O and HEPES buffer.

Furthermore, the interference studies have been performed to ascertain the high affinity of **5** for Hg^{2+}. Upon addition of tested cations (in excess, 20 equiv) to a solution of probable complex, **5**−Hg^{2+} and reversibly, addition of Hg^{2+} to a solution of **5** containing excess of tested cations both the absorption and emission spectra showed insignificant change and the color of solution remained persistent to a blue-green (Figure 1 and Figure S11 in the Supporting Information). Additionally, we separately tested the affinity of **5** toward biologically relevant specific metal ions (M^{n+}) like Fe^{2+}, Fe^{3+}, Mg^{2+}, Ca^{2+}, Zn^{2+} under similar condition. Notably, the emission spectra of **5** upon interaction with M^{n+} ions revealed insignificant sensitivity and selectivity. However, a marginal interference (∼5−7%) of Fe^{3+} occurred in which emission intensity of **5** + Hg^{2+} decreased by only 1−1.5% in comparison to Hg^{2+} (Figure S12 in the Supporting Information).

The reversible mode of complexation between **5** and Hg^{2+} has been realized by the addition of a strong chelating reagent, EDTA, to a solution of a probable complex, **5**−Hg^{2+}. Notably, the revived emission intensity was found almost close to the intensity of **5** probably, due to strong binding affinity of EDTA with Hg^{2+}.[17] The observed marginal rise in emission intensity of **5** upon addition of EDTA (in excess) is attributable to the acidic nature of EDTA and further addition of Hg^{2+} in excess did not reflect any considerable change in the emission behavior of **5**. On repeating this process, the emission behavior of **5** was found nearly consistent for almost 10 cycles (Figure S13 in the Supporting Information). The emission titration experiment was performed to understand the binding affinity of **5** with Hg^{2+} ions. Notably, upon increasing the concentration of Hg^{2+} (0−5 equiv) to a solution of **5**, the fluorescence intensity enhances, "turn-on" gradually, and about ∼10.5-fold maximum fluorescence intensity observed with a red shift of 2−4 nm (Figure 2). Job's plot analysis revealed a 1:2 binding stoichiometry between **5** and Hg^{2+} (inset of Figure 2). The emission titration data was utilized to estimate the association constant for a 1:2 stoichiometry by the B−H method and was found to be 1.06 × $10^{10}/M^2$ (Figure S14 in the Supporting Information) and accordingly the quantum yield was enhanced about ∼13-fold ($\Phi_{5+Hg^{2+}}$ = 0.014). Additionally, the limit of detection (LOD) of **5** to detect Hg^{2+} ions was estimated (Figure S15 in the Supporting Information) in HEPES buffer by our previously reported method.[18−20] The estimated 10 nM (2 ppb) LOD was found comparable to other reported methods and well in limit, suggested by EPA. Thus, **5** shows promise for sensitive and selectivity detection of Hg^{2+}.

Nature of Interaction. In an endeavor to explain the mode of interaction, the ^1H NMR, FT-IR, and mass spectra of the probe **5** and its complex, **5** + Hg^{2+} were analyzed. The multiplet appeared at δ 8.49 and 7.51 ppm and at δ 7.36−7.16 ppm are

dx.doi.org/10.1021/ac501780z | Anal. Chem. 2014, 86, 8693−8699

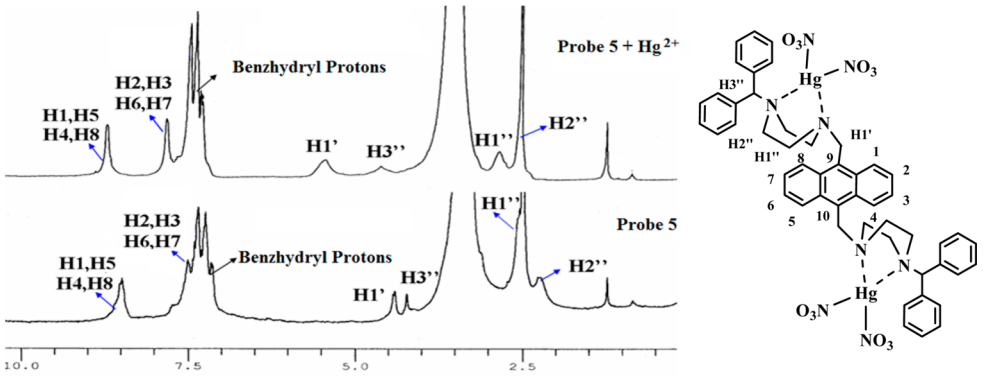

Figure 3. Stacked ^{1}HNMR spectra of **5** and **5** + Hg^{2+} in DMSO-d_6 and a possible mode of interaction between **5** and Hg^{2+}.

attributable to resonances of anthracene (H1,H4,H5,H8 and H2,H3,H6,H7) and benzhydryl unit protons of **5**, respectively (Figure 3 and Figure S5b in the Supporting Information). Similarly, resonances appeared at δ 4.41 and 4.23 ppm have been assigned to $-CH_2$ (H1′) and −CH (H3″) protons while the piperazine unit protons ($-CH_2$; H1″ and H2″) appeared at δ 2.54 and 2.27 ppm, respectively. In contrast, the ^{1}HNMR spectra of a probable complex, **5** + Hg^{2+} exhibited significant downfield shifts wherein anthracene unit protons shifted downfield ($\Delta\delta$ = 0.14 and 0.68 ppm) to appear at δ 8.63 and 8.19 ppm (Figure 3). Similarly, H1′, H3″ and H1″, H2″ resonances shifted downfield ($\Delta\delta$ = 0.97, 0.33 and 0.26, 0.22 ppm) to appear at δ 5.38, 4.56 and 2.80, 2.49 ppm, respectively. The downfield shifts corresponding to the benzhydryl ring protons was relatively less ($\Delta\delta$ = 0.01−0.04 ppm). The FT-IR spectrum of **5** showed characteristic stretching vibration bands at 2961, 2801, 1598, 1492, 1447 and 1331, 1261, 1136, 1095, 1004, 803, 743, and 704 cm^{-1} corresponding to C−H, C═C, C−N, and C−H (Ar) functions (Figure S16 in the Supporting Information). Upon interaction with Hg^{2+}, the C−N stretching vibration band blue-shifted to appear at 1261, 1144, 1110, and 1088 cm^{-1}. The bands appeared at 636 and 626 cm^{-1} suggested about an Hg−N interaction.[21] Moreover, the HRMS spectra of **5** (Figure S7b in the Supporting Information) showed a molecular ion peak, m/z at 707.4067 (calcd 707.4069) which upon complexation with Hg^{2+} changed to appear at 1358.2958 (calcd 1358.2961) (Figure S17 in the Supporting Information). Thus, the observed downfield shifts and typical change in ^{1}HNMR spectral pattern of a complex, **5** + Hg^{2+} along with change in FT-IR and HRMS spectra clearly supported the interaction of probe **5** with Hg^{2+} through the N atoms of piperazine units in 1:2 stoichiometry.

Analytical Application of Probe 5. *Detection of Hg^{2+} in Real Contaminated Water Samples.* To validate practical analytical utility of **5** to determine Hg^{2+} ion concentration in real contaminated water samples, we first quantified the fluorescence of probe **5** (10 μM) in the presence of various concentrations of Hg^{2+} ions (0−8 μM), and the corresponding calibration plot was prepared as the standard curve (Figure 4a). Considering the possible interference of other components present in real samples, the level of Hg^{2+} in real water samples was determined using the standard addition method.[22,23] Prior to real sample detection when **5** was added directly to the water samples, no significant fluorescence enhancement occurred. However, when the emission spectra of treated contaminated water samples were acquired, the recovery of Hg^{2+} with respect to the standard calibration curve was excellent and we could

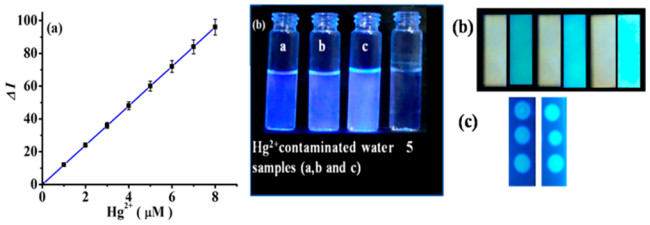

Figure 4. (a) Calibration sensitivity plot of **5** for Hg^{2+} and (b) change in color of **5** and **5** + Hg^{2+} solution (a = 0.02, b = 0.2, c = 2 μM) in HEPES buffer and change in color of **5** and **5**−Hg^{2+} on (c) cellulose paper strips and (d) silica coated slides.

quantify recovered Hg^{2+} contamination in real water samples within the range of 115 to 92% (Table 1), wherein the color of

Table 1. Estimation of Hg^{2+} in Real Water Samples

sample concentration (μM)	Hg^{2+} recovered	% recovery of Hg^{2+} from the sample
0	not detected	
0.02	0.023 ± 0.014	115
0.2	0.19 ± 0.021	95
2	1.84 ± 0.12	92

solutions changed from a fluorescent blue to a blue-green, which was easy to visualize with the naked-eye (Figure 4b). Thus, it is noteworthy to mention that probe **5** has potential to detect mercury contamination in the environment with high sensitivity and selectivity.

Detection of Hg^{2+} on Paper Strips and Silica Coated Slides. We also performed experiments for a colorimetric detection of Hg^{2+} on solid surfaces, such as paper strips and silica coated slides, with varying concentrations of probe **5** and Hg^{2+} solution (please see the Supporting Information). Interestingly, the naked-eye sensitive color of paper strips of probe **5** upon interaction with Hg^{2+} changed from a light yellow to light blue green color under UV light (Figure 4c). Similarly, the probe adsorbed on silica coated slides after interaction with Hg^{2+} showed an immediate naked-eye sensitive color change from a dark blue to a fluorescent blue-green under UV light (Figure 4d).

*Affinity of Probe **5** to Detect Hg^{2+} in Blood Plasma Protein.* The potential applicability of probe **5** to detect Hg^{2+} in a biological medium, such as a blood plasma protein (bovine serum albumin, BSA), has also been studied. Our own research work and others have shown previously that BSA has high affinity for Hg^{2+} ions.[18−20,24] The presence of tryptophan

dx.doi.org/10.1021/ac501780z | Anal. Chem. 2014, 86, 8693−8699

domains[25] in BSA (50 mM NaOAc buffer, pH 6.7) exhibit strong emission at ~345 nm (at λ_{ex} = 278 nm) (Figure S18 in the Supporting Information). However, upon interaction with Hg^{2+} (0–220 μM), about ~83% fluorescence quenching ocuurs with an emission maxima at 345 nm (blue-shift, ~8 nm to appear at 337 nm) (Figure S16 in the Supporting Information). In contrast, the emission behavior of **5** remained independent to even a high concentration of BSA (2 μM) (Figure S19a in the Supporting Information). Thus, the possibilities such as H-bonding and/or electrostatic interactions with blood plasma protein is ruled out. However, addition of Hg^{2+} (5.0 equiv) to a solution of **5** + BSA (10 μM probe; 2 μM BSA, pH 7.0) displayed enhanced turn-on emission (~10-fold) and was almost close to the intensity of **5** + Hg^{2+} without BSA (Figure S19b in the Supporting Information). Moreover, a preliminary observation made in the presence of thiol containing amino acids, such as cysteine (Cys), suggested that the emission behavior of **5** upon interaction with Cys (100 equiv) before and/or after the interaction with Hg^{2+} remained unaffected in HEPES buffer (Figure S20 in the Supporting Information). Thus, it is important to mention that probe **5** has the potential to detect Hg^{2+} in biological samples.

Detection of Hg^{2+} in Living Cells. To study the ability of probe **5** to permeate cells and detect Hg^{2+} *in vivo* and in biological samples, live cell imaging experiments have been performed in HeLa cells through confocal fluorescence microscopy. The cells were first incubated directly with different concentrations of **5** (10, 20, 30, 40, 50 μM) and after proper washing with 1× PBS buffer (phosphate saline, pH 7.4) visualized under a microscope. The observed bright blue color fluorescence indicated excellent permeability of **5** in HeLa cells (Figure 5, images A, B, and C).

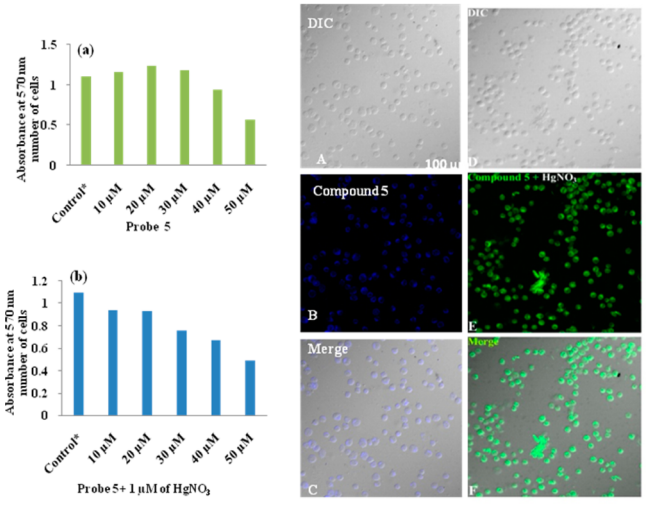

Figure 5. MTT assay for (a) **5** and (b) **5** + $HgNO_3$. Confocal fluorescence images show localization of **5** (blue; panel B) and **5**–Hg^{2+} (green; panel E) in HeLa cells. DIC images of HeLa cells (panels A and D). Merge fluorescence images for **5** and **5** + Hg^{2+} (panels C and F; scale bar, 100 μm).

The MTT assay was performed to understand cell viability and cytotoxic tolerance of HeLa cells corresponding to different concentration of **5** as well as a complex, **5** + Hg^{2+}. The MTT assay experiment implicated that more than 50% cells were viable up to 40 μM concentration of **5** and its complex, **5** + $HgNO_3$ (Figure 5a,b). Therefore, 40 μM concentration was chosen as an optimum concentration to incubate HeLa cells separately in the dark. The confocal microscopic images acquired at 380 nm excitation displayed enhanced green fluorescence for the incubated HeLa cells with **5** + Hg^{2+} in which the relative emission intensity was more intense compared to HeLa cells with probe **5** (Figure 5, images D, E, and F).

Furthermore, to address the minimum possibility of interference of abundantly available PO_4^{3-} ions studies in live cells were performed in the presence of some biologically relevant hard metal ions[26] (M^{n+}) including Hg^{2+} and as a control in the presence of a cell permeable transition metal ion chelator,[27] TPEN (*N*,*N*,*N*′,*N*′-tetrakis(2-pyridylmethyl)-ethylenediamine). The HeLa cells were incubated separately, with probe **5** + M^{n+} ions (5 μM), **5** + M^{n+} + Hg^{2+} (1 μM), and **5** + M^{n+} + Hg^{2+} + TPEN (50 μM) and after proper washing with 1× PBS buffer visualized under a confocal microscope at 380 nm excitation (Figure S21 in the Supporting Information). The HeLa cells incubated with **5** + Hg^{2+} + M^{n+} displayed relatively more intense enhanced green fluorescence (Figure S21 in the Supporting Information, images D and E). However, the incubated HeLa cells containing metal chelator, TPEN (**5** + M^{n+} + Hg^{2+} + TPEN) show diminished emission (Figure S21 in the Supporting Information, image F). The live cell imaging experiments clearly showed potential application of probe **5** to detect Hg^{2+} with high sensitivity and reversibility (with TPEN) in biological samples. Moreover, the presence of specific metal ions (M^{n+}) is expected to minimize the interference of PO_4^{3-} ions inside the live cells.

Response of Probe 5 with Anions. We also checked the applicability of probe **5** to sense the anions in HEPES buffer. Probe **5** as such was found insensitive to anion since no considerable change in fluorescence behavior of **5** occurred upon interaction with different classes of anions (50 equiv) like F^-, Cl^-, Br^-, I^-, OAc^-, CN^-, ClO_4^-, HSO_4^-, NO_3^-, and PO_4^{3-} (Figure S22 in the Supporting Information). However, in HEPES buffer interaction studies of a complex, **5**–Hg^{2+} showed high selectivity only for PO_4^{3-} among the tested anions (5 equiv, sodium salts) (Figure 6), wherein enhanced emission of

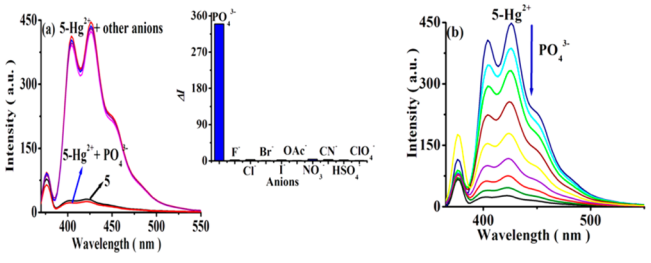

Figure 6. (a) Emission spectra and bar diagram of **5**–Hg^{2+} upon interaction with different anions and (b) emission titration spectra of **5**–Hg^{2+} upon addition of PO_4^{3-}ions (0–5 equiv) in HEPES buffer.

a complex, **5**–Hg^{2+}, diminished almost close to intensity of **5**, probably due to interaction of Hg^{2+} with PO_4^{3-} ions.[28] Furthermore, it is interesting to mention that intensity of **5** remained unaffected upon interaction with PO_4^{3-} in the presence of hard metal ions[26] (M^{n+}), while a further addition of Hg^{2+} (2.5 equiv) to the same solution led to significant fluorescence enhancement (Figure S23 in the Supporting Information). This indicates that the expected binding reversibility of **5** + Hg^{2+} by PO_4^{3-} is inhibited with persistent

dx.doi.org/10.1021/ac501780z | *Anal. Chem.* 2014, 86, 8693–8699

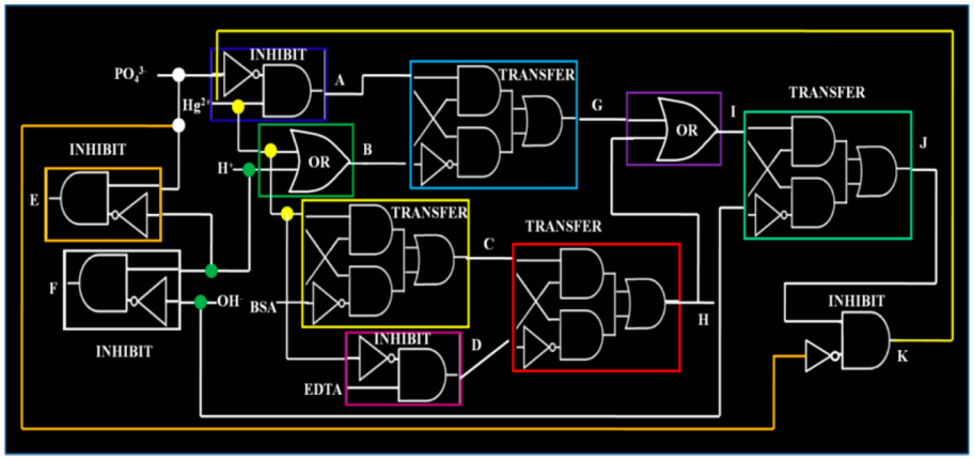

Figure 7. Multiple logic gates and combinational circuit exhibited by **5** upon applying six different chemical inputs of Hg^{2+}, H^+, OH^-, BSA, PO_4^{3-}, and EDTA in HEPES buffer.

enhanced fluorescence and the expected quenching in solution and live cells would remain dogmatic, consequently.

Logic Interpretation. Recently, researchers are trying to mimic the function of silicon chips and building electronic devices based on optoelectronic responses of organic/inorganic molecules in the presence of external stimuli.[29,30] The molecular scaffolds that displays sensitive optical behavior (output) and transform macroscopic properties according to logic operations in the presence of chemical/photonic inputs are in high demand to develop tunable miniaturized electronic devices, fluorescent logic gates and arranged logic circuits.[31−36] The functional fluorescent molecular scaffolds that enable multiple 2-bit Boolean logics from the same initial state are limited in number,[37] and the combination of individual multiple logic systems for their possible use as a unimolecular system has great futuristic applications, particularly in the field of molecular switches.[38,39] Moreover, the reset capacity of functional organic molecules with arithmetic functions stimulate further potential to create a low-dimensional computing devices.[40]

To create logic circuits according to the truth tables, digital values has been assigned as binary numerals, "1" and "0" to illustrate high and low emission outputs as well as applied inputs (present 1; absent 0), respectively. Comparatively, 75% of the maximum output emission intensity was chosen as a threshold value. Notably, **5** upon applying chemical inputs of Hg^{2+} and/or H^+ ion exhibited a maximum emission intensity (high output). In a truth table, outputs emission which are 75% or above the maximum has been considered high (1) and low (0), respectively. The optoelectronic properties of **5** displayed ON-OFF switching behavior in the presence of applied chemical inputs, such as PO_4^{3-} (In_1), Hg^{2+} (In_2), H^+ (In_3), EDTA (In_4), OH^- (In_5), and BSA (In_6), and the respective truth tables (inset of Figures S24−S29 in the Supporting Information) corresponds to different logic gates as INHIBIT, TRANSFER, and OR under respective conditions.

Further, an arranged combinational logic circuit has been constructed by the combination of outputs of different logic gates in a unimolecular system (Figure 7). A combination of outputs (A and B) of two logic gates INHIBIT and OR as inputs (In_7 and In_8) gave a new TRANSFER gate (output "G") as the absence of both inputs or presence of only In_7 exhibit low emission while the presence of both or only In_8 give high output emission. Similarly, when the outputs (C and D) of two gates TRANSFER and INHIBIT were utilized as inputs (In_9 and In_{10}) truth table (Table S1 in the Supporting Information) corresponds to a new TRANSFER (output "H") gate. Now a combination of two outputs (G and H) outfitted a new OR gate (output "I"). In this case, the absence of both shows low fluorescence (output state "0") while the presence of either or both generates the high fluorescence (output state "1") (Figure 7). Moreover, we could reset output emission of our resultant combinational circuit to the low fluorescence state by applying two reset keys (as OH^- and PO_4^{3-}). When the reset key in the form of OH^- is applied as input along with output "I" of OR gate led to a TRANSFER gate (output "J"), as the OH^- neutralize the effect of H^+ but since Hg^{2+} is present, the emission of probe **5** remained in the switched ON-state. Interestingly, utilizing output "J" as input along with PO_4^{3-} reset the circuit to original low emission switched-OFF state (turn-ON → turn-OFF) and regenerate an INHIBIT gate (output "K"). Now the constructed combinational circuit based on the emission behavior of **5** is ready for further use (Figure 7). It is important to mention that we could perform the set-reset operation 3−5 times without considerable loss in emission properties of the probe **5** under the condition.

■ CONCLUSION

Conclusively through this contribution we have demonstrated the design and synthesis of an efficient photoinduced electron transfer (PET) fluorescent probe **5**. Probe **5** has shown good real time fluorescence "turn-ON" response, high sensitivity, and considerable selectivity to detect Hg^{2+} in partial aqueous medium, on paper strips, silica coated microslides, and in real water samples. Probe **5** has shown high cell permeability and low toxicity to detect Hg^{2+} sensitively *in vivo* as well as in protein medium. The high limit of detection (2 ppb) with recovery in the range of 90−115% has predicted the potential application of **5** to sense Hg^{2+} in biological and environmental samples. Moreover, the excellent optoelectronic properties of **5** providing different chemical inputs has been utilized to create a reusable combinational logic circuit and suitable optoelectronic devices such as molecular logic switches.

dx.doi.org/10.1021/ac501780z | *Anal. Chem.* 2014, 86, 8693−8699

■ ASSOCIATED CONTENT

Supporting Information

Experimental details, synthesis, ^{1}HNMR, ^{13}CNMR, FT-IR, ESI-MS, UV−Vis, and fluorescence spectra. This material is available free of charge via the Internet at http://pubs.acs.org.

■ AUTHOR INFORMATION

Corresponding Author

*Phone: +91-0542-2307321 ext. 104; +91-0542-6702503. Fax: +91-0542-2368127; +91-0542-2368175. E-mail: arvindmisra2003@yahoo.com; amisra@bhu.ac.in.

Notes

The authors declare no competing financial interest.

§The authors have performed experiments in live cells.

■ ACKNOWLEDGMENTS

The authors are thankful to CSIR, New Delhi, India for funding and fellowships (SRF to P.S., S.S.R., R.A. and UGC-JRF to R.C.G.) to carry out the research work. We are also thankful to the Head of the Department of Chemistry, Faculty of Science, Banaras Hindu University for creating the necessary facilities to carry out the advanced research studies.

■ REFERENCES

(1) Clarkson, T. W.; Magos, L.; Myers, G. J. *N. Engl. J. Med.* **2003**, *349*, 1731−1737.

(2) Nolan, E. M.; Lippard, S. J. *Chem. Rev.* **2008**, *108*, 3443−3480.

(3) Kim, H. N.; Ren, W. X.; Kim, J. S.; Yoon, J. *Chem. Soc. Rev.* **2012**, *41*, 3210−3244.

(4) Koziar, J. C.; Cowan, D. O. *Acc. Chem. Res.* **1978**, *11*, 334−341.

(5) Lee, M. H.; Cho, B.-K.; Yoon, J.; Kim, J. S. *Org. Lett.* **2007**, *9*, 4515−4518.

(6) Du, J.; Hu, M.; Fan, J.; Peng, X. *Chem. Soc. Rev.* **2012**, *41*, 4511−4535.

(7) Chen, X.; Pradhan, T.; Wang, F.; Kim, J. S.; Yoon, J. *Chem. Rev.* **2012**, *112*, 1910−1956.

(8) Huang, J.; Xu, Y.; Qian, X. *J. Org. Chem.* **2009**, *74*, 2167−2170.

(9) Yoon, S.; Albers, A. E.; Wong, A. P.; Chang, C. *J. Am. Chem. Soc.* **2005**, *127*, 16030−16031.

(10) Khatua, S.; Schmittel, M. *Org. Lett.* **2013**, *15*, 4422−4425.

(11) Bera, K.; Das, A. K.; Nag, M.; Basak, S. *Anal. Chem.* **2014**, *86*, 2740−2746.

(12) Singh, A.; Raj, T.; Aree, T.; Singh, N. *Inorg. Chem.* **2013**, *52*, 13830−13832.

(13) Yang, Z.; Hao, L.; Yin, B.; She, M.; Obst, M.; Kappler, A.; Li, J. *Org. Lett.* **2013**, *15*, 4334−4337.

(14) Nolte, M.; Pantenburg, I.; Meyer, G. *Z. Anorg. Allg. Chem.* **2005**, *631*, 2923−2927.

(15) de Silva, A. P.; Moody, T. S.; Wright, G. D. *Analyst* **2009**, *134*, 2385−2393.

(16) Wang, C.; Wong, K. M-C. *Inorg. Chem.* **2013**, *52*, 13432−13441.

(17) Schwarzenbach, G. In *Comprehensive Titrations*; Chapman and Hall: London, 1957.

(18) Misra, A.; Srivastava, P.; Shahid, M. *Analyst* **2012**, *137*, 3470−3478.

(19) Srivastava, P.; Shahid, M.; Misra, A. *Org. Biomol. Chem.* **2011**, *9*, 5051−5055.

(20) Srivastava, P.; Ali, R.; Razi, S. S.; Shahid, M.; Misra, A. *Sens. Actuators, B* **2013**, *181*, 584−595.

(21) Misra, A.; Shahid, M. *J. Phys. Chem. C* **2010**, *114*, 16726−16739.

(22) Li, J.; Zhang, C.-F.; Yang, S.-H.; Yang, W.-C.; Yang, G.-F. *Anal. Chem.* **2014**, *86*, 3037−3042.

(23) Wang, Z.; Han, D. M.; Jia, W. P.; Zhou, Q. Z.; Deng, W. P. *Anal. Chem.* **2012**, *84*, 4915−4920.

(24) Ma, L.-J.; Li, Y.; Li, L.; Sun, J.; Tian, C.; Wu, Y. *Chem. Commun.* **2008**, 6345−6347.

(25) Yamasaki, K.; Maruyama, T.; Kragh-Hansen, U.; Otagiri, M. *Biochim. Biophys. Acta* **1996**, *1295*, 147−157.

(26) Pearson, R. G. *J. Am. Chem. Soc.* **1963**, *85*, 3533−3539.

(27) Huang, J.; Xua, Y.; Qian, X. *Dalton Trans.* **2014**, *43*, 5983−5989.

(28) Saluja, P.; Kaur, N.; Singh, N.; Jang, D. O. *Tetrahedron Lett.* **2012**, *53*, 3292−3295.

(29) Szacilowski, K. *Chem. Rev.* **2008**, *108*, 3481−3548.

(30) Andreasson, J.; Pischel, U. *Chem. Soc. Rev.* **2010**, *39*, 174−188.

(31) Balzini, V.; Venturi, M.; Credi, A. *Molecular Devices and Machines: A Journey into the Nano World*; Wiley-VCH: Weinheim, Germany, 2003.

(32) Kou, S.; Lee, H. N.; van Noort, D.; Swamy, K. M. K.; Kim, S. H.; Soh, J. H.; Lee, K.-M.; Nam, S.-W.; Yoon, J.; Park, S. *Angew. Chem., Int. Ed.* **2008**, *47*, 872−876.

(33) Pathak, R. K.; Dessingou, J.; Hinge, V. K.; Thawari, A. G.; Basu, S. K.; Pulla Rao, C. *Anal. Chem.* **2013**, *85*, 3707−3714.

(34) Pu, S.; Ding, H.; Liu, G.; Zheng, C.; Xu, H. *J. Phys. Chem. C* **2014**, *118*, 7010−7017.

(35) Raymo, F. M. *Adv. Mater.* **2002**, *14*, 401−414.

(36) de Silva, A. P.; James, M. R.; Mckinney, B. D.; Pears, D. A.; Weir, S. M. *Nat. Mater.* **2006**, *5*, 787−789.

(37) Fang, C. J.; Zhu, Z.; Sun, W.; Xu, C. H.; Yan, C. H. *New J. Chem.* **2007**, *31*, 580−586.

(38) Strack, G.; Ornatska, M.; Pita, M.; Katz, E. *J. Am. Chem. Soc.* **2008**, *130*, 4234−4235.

(39) Coskun, A.; Deniz, E.; Akkaya, E. U. *Org. Lett.* **2005**, *7*, 5187−5189.

(40) Margulies, D.; Melman, G.; Shanzer, A. *J. Am. Chem. Soc.* **2006**, *128*, 4865−4871.